Evidence for the decay X(3872) -> J/psi omega

del Amo Sanchez, P.; Raven, H.G.; Snoek, H.

published in
Physical Review D
2010

DOI (link to publisher)
10.1103/PhysRevD.82.011101

document version
Publisher's PDF, also known as Version of record

PHYSICAL REVIEW D **82,** 011101(R) (2010)

Evidence for the decay $X(3872) \to J/\psi\omega$

P. del Amo Sanchez,[1] J. P. Lees,[1] V. Poireau,[1] E. Prencipe,[1] V. Tisserand,[1] J. Garra Tico,[2] E. Grauges,[2] M. Martinelli,[3a,3b] A. Palano,[3a,3b] M. Pappagallo,[3a,3b] G. Eigen,[4] B. Stugu,[4] L. Sun,[4] M. Battaglia,[5] D. N. Brown,[5] B. Hooberman,[5] L. T. Kerth,[5] Yu. G. Kolomensky,[5] G. Lynch,[5] I. L. Osipenkov,[5] T. Tanabe,[5] C. M. Hawkes,[6] A. T. Watson,[6] H. Koch,[7] T. Schroeder,[7] D. J. Asgeirsson,[8] C. Hearty,[8] T. S. Mattison,[8] J. A. McKenna,[8] A. Khan,[9] A. Randle-Conde,[9] V. E. Blinov,[10] A. R. Buzykaev,[10] V. P. Druzhinin,[10] V. B. Golubev,[10] A. P. Onuchin,[10] S. I. Serednyakov,[10] Yu. I. Skovpen,[10] E. P. Solodov,[10] K. Yu. Todyshev,[10] A. N. Yushkov,[10] M. Bondioli,[11] S. Curry,[11] D. Kirkby,[11] A. J. Lankford,[11] M. Mandelkern,[11] E. C. Martin,[11] D. P. Stoker,[11] H. Atmacan,[12] J. W. Gary,[12] F. Liu,[12] O. Long,[12] G. M. Vitug,[12] C. Campagnari,[13] T. M. Hong,[13] D. Kovalskyi,[13] J. D. Richman,[13] A. M. Eisner,[14] C. A. Heusch,[14] J. Kroseberg,[14] W. S. Lockman,[14] A. J. Martinez,[14] T. Schalk,[14] B. A. Schumm,[14] A. Seiden,[14] L. O. Winstrom,[14] C. H. Cheng,[15] D. A. Doll,[15] B. Echenard,[15] D. G. Hitlin,[15] P. Ongmongkolkul,[15] F. C. Porter,[15] A. Y. Rakitin,[15] R. Andreassen,[16] M. S. Dubrovin,[16] G. Mancinelli,[16] B. T. Meadows,[16] M. D. Sokoloff,[16] P. C. Bloom,[17] W. T. Ford,[17] A. Gaz,[17] M. Nagel,[17] U. Nauenberg,[17] J. G. Smith,[17] S. R. Wagner,[17] R. Ayad,[18,*] W. H. Toki,[18] T. M. Karbach,[19] J. Merkel,[19] A. Petzold,[19] B. Spaan,[19] K. Wacker,[19] M. J. Kobel,[20] K. R. Schubert,[20] R. Schwierz,[20] D. Bernard,[21] M. Verderi,[21] P. J. Clark,[22] S. Playfer,[22] J. E. Watson,[22] M. Andreotti,[23a,23b] D. Bettoni,[23a] C. Bozzi,[23a] R. Calabrese,[23a,23b] A. Cecchi,[23a,23b] G. Cibinetto,[23a,23b] E. Fioravanti,[23a,23b] P. Franchini,[23a,23b] E. Luppi,[23a,23b] M. Munerato,[23a,23b] M. Negrini,[23a,23b] A. Petrella,[23a,23b] L. Piemontese,[23a] R. Baldini-Ferroli,[24] A. Calcaterra,[24] R. de Sangro,[24] G. Finocchiaro,[24] M. Nicolaci,[24] S. Pacetti,[24] P. Patteri,[24] I. M. Peruzzi,[24,†] M. Piccolo,[24] M. Rama,[24] A. Zallo,[24] R. Contri,[25a,25b] E. Guido,[25a,25b] M. Lo Vetere,[25a,25b] M. R. Monge,[25a,25b] S. Passaggio,[25a] C. Patrignani,[25a,25b] E. Robutti,[25a] S. Tosi,[25a,25b] B. Bhuyan,[26] C. L. Lee,[27] M. Morii,[27] A. Adametz,[28] J. Marks,[28] S. Schenk,[28] U. Uwer,[28] F. U. Bernlochner,[29] M. Ebert,[29] H. M. Lacker,[29] T. Lueck,[29] A. Volk,[29] P. D. Dauncey,[30] M. Tibbetts,[30] P. K. Behera,[31] U. Mallik,[31] C. Chen,[32] J. Cochran,[32] H. B. Crawley,[32] L. Dong,[32] W. T. Meyer,[32] S. Prell,[32] E. I. Rosenberg,[32] A. E. Rubin,[32] Y. Y. Gao,[33] A. V. Gritsan,[33] Z. J. Guo,[33] N. Arnaud,[34] M. Davier,[34] D. Derkach,[34] J. Firmino da Costa,[34] G. Grosdidier,[34] F. Le Diberder,[34] A. M. Lutz,[34] B. Malaescu,[34] A. Perez,[34] P. Roudeau,[34] M. H. Schune,[34] J. Serrano,[34] V. Sordini,[34,‡] A. Stocchi,[34] L. Wang,[34] G. Wormser,[34] D. J. Lange,[35] D. M. Wright,[35] I. Bingham,[36] C. A. Chavez,[36] J. P. Coleman,[36] J. R. Fry,[36] E. Gabathuler,[36] R. Gamet,[36] D. E. Hutchcroft,[36] D. J. Payne,[36] C. Touramanis,[36] A. J. Bevan,[37] F. Di Lodovico,[37] R. Sacco,[37] M. Sigamani,[37] G. Cowan,[38] S. Paramesvaran,[38] A. C. Wren,[38] D. N. Brown,[39] C. L. Davis,[39] A. G. Denig,[40] M. Fritsch,[40] W. Gradl,[40] A. Hafner,[40] K. E. Alwyn,[41] D. Bailey,[41] R. J. Barlow,[41] G. Jackson,[41] G. D. Lafferty,[41] T. J. West,[41] J. Anderson,[42] R. Cenci,[42] A. Jawahery,[42] D. A. Roberts,[42] G. Simi,[42] J. M. Tuggle,[42] C. Dallapiccola,[43] E. Salvati,[43] R. Cowan,[44] D. Dujmic,[44] P. H. Fisher,[44] G. Sciolla,[44] M. Zhao,[44] D. Lindemann,[45] P. M. Patel,[45] S. H. Robertson,[45] M. Schram,[45] P. Biassoni,[46a,46b] A. Lazzaro,[46a,46b] V. Lombardo,[46a] F. Palombo,[46a,46b] S. Stracka,[46a,46b] L. Cremaldi,[47] R. Godang,[47,§] R. Kroeger,[47] P. Sonnek,[47] D. J. Summers,[47] X. Nguyen,[48] M. Simard,[48] P. Taras,[48] G. De Nardo,[49a,49b] D. Monorchio,[49a,49b] G. Onorato,[49a,49b] C. Sciacca,[49a,49b] G. Raven,[50] H. L. Snoek,[50] C. P. Jessop,[51] K. J. Knoepfel,[51] J. M. LoSecco,[51] W. F. Wang,[51] L. A. Corwin,[52] K. Honscheid,[52] R. Kass,[52] J. P. Morris,[52] A. M. Rahimi,[52] N. L. Blount,[53] J. Brau,[53] R. Frey,[53] O. Igonkina,[53] J. A. Kolb,[53] R. Rahmat,[53] N. B. Sinev,[53] D. Strom,[53] J. Strube,[53] E. Torrence,[53] G. Castelli,[54a,54b] E. Feltresi,[54a,54b] N. Gagliardi,[54a,54b] M. Margoni,[54a,54b] M. Morandin,[54a] M. Posocco,[54a] M. Rotondo,[54a] F. Simonetto,[54a,54b] R. Stroili,[54a,54b] E. Ben-Haim,[55] G. R. Bonneaud,[55] H. Briand,[55] G. Calderini,[55] J. Chauveau,[55] O. Hamon,[55] Ph. Leruste,[55] G. Marchiori,[55] J. Ocariz,[55] J. Prendki,[55] S. Sitt,[55] M. Biasini,[56a,56b] E. Manoni,[56a,56b] A. Rossi,[56a,56b] C. Angelini,[57a,57b] G. Batignani,[57a,57b] S. Bettarini,[57a,57b] M. Carpinelli,[57a,57b,‖] G. Casarosa,[57a,57b] A. Cervelli,[57a,57b] F. Forti,[57a,57b] M. A. Giorgi,[57a,57b] A. Lusiani,[57a,57c] N. Neri,[57a,57b] E. Paoloni,[57a,57b] G. Rizzo,[57a,57b] J. J. Walsh,[57a] D. Lopes Pegna,[58] C. Lu,[58] J. Olsen,[58] A. J. S. Smith,[58] A. V. Telnov,[58] F. Anulli,[59a] E. Baracchini,[59a,59b] G. Cavoto,[59a] R. Faccini,[59a,59b] F. Ferrarotto,[59a] F. Ferroni,[59a,59b] M. Gaspero,[59a,59b] L. Li Gioi,[59a] M. A. Mazzoni,[59a] G. Piredda,[59a] F. Renga,[59a,59b] T. Hartmann,[60] T. Leddig,[60] H. Schröder,[60] R. Waldi,[60] T. Adye,[61] B. Franek,[61] E. O. Olaiya,[61] F. F. Wilson,[61] S. Emery,[62] G. Hamel de Monchenault,[62] G. Vasseur,[62] Ch. Yèche,[62] M. Zito,[62] M. T. Allen,[63] D. Aston,[63] D. J. Bard,[63] R. Bartoldus,[63] J. F. Benitez,[63] C. Cartaro,[63] M. R. Convery,[63] J. Dorfan,[63] G. P. Dubois-Felsmann,[63] W. Dunwoodie,[63] R. C. Field,[63] M. Franco Sevilla,[63] B. G. Fulsom,[63] A. M. Gabareen,[63] M. T. Graham,[63] P. Grenier,[63] C. Hast,[63] W. R. Innes,[63] M. H. Kelsey,[63] H. Kim,[63] P. Kim,[63] M. L. Kocian,[63] D. W. G. S. Leith,[63] S. Li,[63] B. Lindquist,[63] S. Luitz,[63] V. Luth,[63] H. L. Lynch,[63] D. B. MacFarlane,[63] H. Marsiske,[63] D. R. Muller,[63] H. Neal,[63] S. Nelson,[63] C. P. O'Grady,[63] I. Ofte,[63] M. Perl,[63] T. Pulliam,[63] B. N. Ratcliff,[63] A. Roodman,[63] A. A. Salnikov,[63] V. Santoro,[63] R. H. Schindler,[63] J. Schwiening,[63]

A. Snyder,[63] D. Su,[63] M. K. Sullivan,[63] S. Sun,[63] K. Suzuki,[63] J. M. Thompson,[63] J. Va'vra,[63] A. P. Wagner,[63] M. Weaver,[63] C. A. West,[63] W. J. Wisniewski,[63] M. Wittgen,[63] D. H. Wright,[63] H. W. Wulsin,[63] A. K. Yarritu,[63] C. C. Young,[63] V. Ziegler,[63] X. R. Chen,[64] W. Park,[64] M. V. Purohit,[64] R. M. White,[64] J. R. Wilson,[64] S. J. Sekula,[65] M. Bellis,[66] P. R. Burchat,[66] A. J. Edwards,[66] T. S. Miyashita,[66] S. Ahmed,[67] M. S. Alam,[67] J. A. Ernst,[67] B. Pan,[67] M. A. Saeed,[67] S. B. Zain,[67] N. Guttman,[68] A. Soffer,[68] P. Lund,[69] S. M. Spanier,[69] R. Eckmann,[70] J. L. Ritchie,[70] A. M. Ruland,[70] C. J. Schilling,[70] R. F. Schwitters,[70] B. C. Wray,[70] J. M. Izen,[71] X. C. Lou,[71] F. Bianchi,[72a,72b] D. Gamba,[72a,72b] M. Pelliccioni,[72a,72b] M. Bomben,[73a,73b] L. Lanceri,[73a,73b] L. Vitale,[73a,73b] N. Lopez-March,[74] F. Martinez-Vidal,[74] D. A. Milanes,[74] A. Oyanguren,[74] J. Albert,[75] Sw. Banerjee,[75] H. H. F. Choi,[75] K. Hamano,[75] G. J. King,[75] R. Kowalewski,[75] M. J. Lewczuk,[75] I. M. Nugent,[75] J. M. Roney,[75] R. J. Sobie,[75] T. J. Gershon,[76] P. F. Harrison,[76] T. E. Latham,[76] E. M. T. Puccio,[76] H. R. Band,[77] X. Chen,[77] S. Dasu,[77] K. T. Flood,[77] Y. Pan,[77] R. Prepost,[77] C. O. Vuosalo,[77] and S. L. Wu[77]

(The *BABAR* Collaboration)

[1]*Laboratoire d'Annecy-le-Vieux de Physique des Particules (LAPP), Université de Savoie, CNRS/IN2P3, F-74941 Annecy-Le-Vieux, France*
[2]*Universitat de Barcelona, Facultat de Fisica, Departament ECM, E-08028 Barcelona, Spain*
[3a]*INFN Sezione di Bari, I-70126 Bari, Italy*
[3b]*Dipartimento di Fisica, Università di Bari, I-70126 Bari, Italy*
[4]*University of Bergen, Institute of Physics, N-5007 Bergen, Norway*
[5]*Lawrence Berkeley National Laboratory and University of California, Berkeley, California 94720, USA*
[6]*University of Birmingham, Birmingham, B15 2TT, United Kingdom*
[7]*Ruhr Universität Bochum, Institut für Experimentalphysik 1, D-44780 Bochum, Germany*
[8]*University of British Columbia, Vancouver, British Columbia, Canada V6T 1Z1*
[9]*Brunel University, Uxbridge, Middlesex UB8 3PH, United Kingdom*
[10]*Budker Institute of Nuclear Physics, Novosibirsk 630090, Russia*
[11]*University of California at Irvine, Irvine, California 92697, USA*
[12]*University of California at Riverside, Riverside, California 92521, USA*
[13]*University of California at Santa Barbara, Santa Barbara, California 93106, USA*
[14]*University of California at Santa Cruz, Institute for Particle Physics, Santa Cruz, California 95064, USA*
[15]*California Institute of Technology, Pasadena, California 91125, USA*
[16]*University of Cincinnati, Cincinnati, Ohio 45221, USA*
[17]*University of Colorado, Boulder, Colorado 80309, USA*
[18]*Colorado State University, Fort Collins, Colorado 80523, USA*
[19]*Technische Universität Dortmund, Fakultät Physik, D-44221 Dortmund, Germany*
[20]*Technische Universität Dresden, Institut für Kern- und Teilchenphysik, D-01062 Dresden, Germany*
[21]*Laboratoire Leprince-Ringuet, CNRS/IN2P3, Ecole Polytechnique, F-91128 Palaiseau, France*
[22]*University of Edinburgh, Edinburgh EH9 3JZ, United Kingdom*
[23a]*INFN Sezione di Ferrara, I-44100 Ferrara, Italy*
[23b]*Dipartimento di Fisica, Università di Ferrara, I-44100 Ferrara, Italy*
[24]*INFN Laboratori Nazionali di Frascati, I-00044 Frascati, Italy*
[25a]*INFN Sezione di Genova, I-16146 Genova, Italy*
[25b]*Dipartimento di Fisica, Università di Genova, I-16146 Genova, Italy*
[26]*Indian Institute of Technology Guwahati, Guwahati, Assam, 781 039, India*
[27]*Harvard University, Cambridge, Massachusetts 02138, USA*
[28]*Universität Heidelberg, Physikalisches Institut, Philosophenweg 12, D-69120 Heidelberg, Germany*
[29]*Humboldt-Universität zu Berlin, Institut für Physik, Newtonstr. 15, D-12489 Berlin, Germany*
[30]*Imperial College London, London, SW7 2AZ, United Kingdom*
[31]*University of Iowa, Iowa City, Iowa 52242, USA*
[32]*Iowa State University, Ames, Iowa 50011-3160, USA*
[33]*Johns Hopkins University, Baltimore, Maryland 21218, USA*
[34]*Laboratoire de l'Accélérateur Linéaire, IN2P3-CNRS et Université Paris-Sud 11, Centre Scientifique d'Orsay, B. P. 34, F-91898 Orsay Cedex, France*
[35]*Lawrence Livermore National Laboratory, Livermore, California 94550, USA*
[36]*University of Liverpool, Liverpool L69 7ZE, United Kingdom*
[37]*Queen Mary, University of London, London, E1 4NS, United Kingdom*
[38]*University of London, Royal Holloway and Bedford New College, Egham, Surrey TW20 0EX, United Kingdom*
[39]*University of Louisville, Louisville, Kentucky 40292, USA*

[40]*Johannes Gutenberg-Universität Mainz, Institut für Kernphysik, D-55099 Mainz, Germany*
[41]*University of Manchester, Manchester M13 9PL, United Kingdom*
[42]*University of Maryland, College Park, Maryland 20742, USA*
[43]*University of Massachusetts, Amherst, Massachusetts 01003, USA*
[44]*Massachusetts Institute of Technology, Laboratory for Nuclear Science, Cambridge, Massachusetts 02139, USA*
[45]*McGill University, Montréal, Québec, Canada H3A 2T8*
[46a]*INFN Sezione di Milano, I-20133 Milano, Italy*
[46b]*Dipartimento di Fisica, Università di Milano, I-20133 Milano, Italy*
[47]*University of Mississippi, University, Mississippi 38677, USA*
[48]*Université de Montréal, Physique des Particules, Montréal, Québec, Canada H3C 3J7*
[49a]*INFN Sezione di Napoli, I-80126 Napoli, Italy*
[49b]*Dipartimento di Scienze Fisiche, Università di Napoli Federico II, I-80126 Napoli, Italy*
[50]*NIKHEF, National Institute for Nuclear Physics and High Energy Physics, NL-1009 DB Amsterdam, The Netherlands*
[51]*University of Notre Dame, Notre Dame, Indiana 46556, USA*
[52]*Ohio State University, Columbus, Ohio 43210, USA*
[53]*University of Oregon, Eugene, Oregon 97403, USA*
[54a]*INFN Sezione di Padova, I-35131 Padova, Italy*
[54b]*Dipartimento di Fisica, Università di Padova, I-35131 Padova, Italy*
[55]*Laboratoire de Physique Nucléaire et de Hautes Energies, IN2P3/CNRS, Université Pierre et Marie Curie-Paris6, Université Denis Diderot-Paris7, F-75252 Paris, France*
[56a]*INFN Sezione di Perugia, I-06100 Perugia, Italy*
[56b]*Dipartimento di Fisica, Università di Perugia, I-06100 Perugia, Italy*
[57a]*INFN Sezione di Pisa, I-56127 Pisa, Italy*
[57b]*Dipartimento di Fisica, Università di Pisa, I-56127 Pisa, Italy*
[57c]*Scuola Normale Superiore di Pisa, I-56127 Pisa, Italy*
[58]*Princeton University, Princeton, New Jersey 08544, USA*
[59a]*INFN Sezione di Roma, I-00185 Roma, Italy*
[59b]*Dipartimento di Fisica, Università di Roma La Sapienza, I-00185 Roma, Italy*
[60]*Universität Rostock, D-18051 Rostock, Germany*
[61]*Rutherford Appleton Laboratory, Chilton, Didcot, Oxon, OX11 0QX, United Kingdom*
[62]*CEA, Irfu, SPP, Centre de Saclay, F-91191 Gif-sur-Yvette, France*
[63]*SLAC National Accelerator Laboratory, Stanford, California 94309 USA*
[64]*University of South Carolina, Columbia, South Carolina 29208, USA*
[65]*Southern Methodist University, Dallas, Texas 75275, USA*
[66]*Stanford University, Stanford, California 94305-4060, USA*
[67]*State University of New York, Albany, New York 12222, USA*
[68]*Tel Aviv University, School of Physics and Astronomy, Tel Aviv, 69978, Israel*
[69]*University of Tennessee, Knoxville, Tennessee 37996, USA*
[70]*University of Texas at Austin, Austin, Texas 78712, USA*
[71]*University of Texas at Dallas, Richardson, Texas 75083, USA*
[72a]*INFN Sezione di Torino, I-10125 Torino, Italy*
[72b]*Dipartimento di Fisica Sperimentale, Università di Torino, I-10125 Torino, Italy*
[73a]*INFN Sezione di Trieste, I-34127 Trieste, Italy*
[73b]*Dipartimento di Fisica, Università di Trieste, I-34127 Trieste, Italy*
[74]*IFIC, Universitat de Valencia-CSIC, E-46071 Valencia, Spain*
[75]*University of Victoria, Victoria, British Columbia, Canada V8W 3P6*
[76]*Department of Physics, University of Warwick, Coventry CV4 7AL, United Kingdom*
[77]*University of Wisconsin, Madison, Wisconsin 53706, USA*
(Received 1 June 2010; published 9 July 2010)

We present a study of the decays $B^{0,+} \to J/\psi \pi^+ \pi^- \pi^0 K^{0,+}$, using 467×10^6 $B\bar{B}$ pairs recorded with the *BABAR* detector. We present evidence for the decay mode $X(3872) \to J/\psi \omega$, with product branching fractions $\mathcal{B}(B^+ \to X(3872)K^+) \times \mathcal{B}(X(3872) \to J/\psi \omega) = [0.6 \pm 0.2(\text{stat}) \pm 0.1(\text{syst})] \times 10^{-5}$, and

*Now at Temple University, Philadelphia, PA 19122, USA
†Also with Università di Perugia, Dipartimento di Fisica, Perugia, Italy
‡Also with Università di Roma La Sapienza, I-00185 Roma, Italy
§Now at University of South Alabama, Mobile, AL 36688, USA
‖Also with Università di Sassari, Sassari, Italy

$\mathcal{B}(B^0 \to X(3872)K^0) \times \mathcal{B}(X(3872) \to J/\psi\omega) = [0.6 \pm 0.3(\text{stat}) \pm 0.1(\text{syst})] \times 10^{-5}$. A detailed study of the $\pi^+\pi^-\pi^0$ mass distribution from $X(3872)$ decay favors a negative-parity assignment.

DOI: 10.1103/PhysRevD.82.011101 PACS numbers: 13.25.Hw, 12.15.Hh, 11.30.Er

The $X(3872)$ meson (denoted in the following as the X meson) has been observed primarily in its $J/\psi\pi^+\pi^-$ decay mode [1–6]. Evidence for its decay to the $J/\psi\gamma$ [7–9] and $\psi(2S)\gamma$ [9] final states has established positive C parity. Analyses by the CDF Collaboration of the $\pi^+\pi^-$ mass distribution [10], and of the decay angular distribution [11], for the $J/\psi\pi^+\pi^-$ decay mode have narrowed the possible spin-parity (J^P) assignment to 1^+ or 2^-. The decay $X \to D^0\bar{D}^0\pi^0$ has also been observed [12] and interpreted as evidence for $X \to D^{*0}\bar{D}^0$; this has been confirmed by subsequent analyses [13,14]. There has been much theoretical interest in the nature of the X meson [15–22]. Hence, additional experimental information on new decay modes, especially those sensitive to the J^P assignment, is germane to the theoretical understanding of this state.

In a previous *BABAR* publication [23], we have confirmed the observation of the $Y(3940)$ meson (denoted in the following as the Y meson) in the decay mode $Y \to J/\psi\omega$ reported by the Belle Collaboration in $B^{0,+} \to J/\psi\omega K^{0,+}$ decay [24]. In the *BABAR* analysis of this decay mode, the $\omega \to \pi^+\pi^-\pi^0$ mass ($m_{3\pi}$) region was defined as $0.7695 \le m_{3\pi} \le 0.7965$ GeV/c^2. With this requirement and the other selection criteria of Ref. [23], we reported no evidence for the decay $X \to J/\psi\omega$, although Monte Carlo (MC) simulation of X-meson decay to an S-wave $J/\psi\omega$ system indicated that this decay could have been observed. An unpublished Belle analysis of $B^+ \to J/\psi\pi^+\pi^-\pi^0K^+$ [7], which required $|m(J/\psi\pi^+\pi^-\pi^0) - 3.872| < 0.0165$ GeV/c^2, reported evidence for the decay $X \to J/\psi\omega$ on the basis of 12.4 ± 4.1 events in the mass interval $0.750 \le m_{3\pi} \le 0.775$ GeV/c^2.

In this study we repeat our analysis of the decay modes $B^{0,+} \to J/\psi\pi^+\pi^-\pi^0K^{0,+}$ [23,25], extending the selected $m_{3\pi}$ region to $0.5 < m_{3\pi} < 0.9$ GeV/c^2 in order to investigate the $m_{3\pi}$ distribution in a broader region around the ω meson.

The data were collected with the *BABAR* detector [26] at the PEP-II asymmetric-energy e^+e^- collider operated at the $\Upsilon(4S)$ resonance. We use the entire integrated luminosity at this center-of-mass (c.m.) energy (~ 426 fb^{-1}), which yields a data sample corresponding to about 467×10^6 $B\bar{B}$ pairs. The entire data sample was reprocessed using the most recent version of the event-reconstruction and particle-identification code.

The event-selection criteria are identical to those in Table I of Ref. [23], except for the initial $m_{3\pi}$ requirement. The B-meson signal region is defined using the c.m. energy difference $\Delta E = E_B^* - \sqrt{s}/2$, and the beam-energy substituted mass $m_{\text{ES}} = \sqrt{[(s/2 + \vec{p}_i \cdot \vec{p}_B)/E_i]^2 - |\vec{p}_B|^2}$ [26], where $(E_i, \vec{p}_i)$ is the initial state four-momentum vector in the laboratory frame, $\sqrt{s}$ is the c.m. energy, E_B^* is the B-meson energy in the c.m., and $\vec{p}_B$ is its laboratory-frame momentum. Signal B^+ (B^0) candidates satisfy $|\Delta E| <$ 20 MeV (15 MeV). In events with multiple B candidates (12% of events in the region $5.274 < m_{\text{ES}} < 5.284$ GeV/c^2), the candidate with the smallest $|\Delta E|$ is chosen.

For the B^+-candidate sample, the $m_{3\pi}$ distribution is shown in Fig. 1. The contribution in each mass interval is obtained by fitting the corresponding m_{ES} distribution in the region $5.2 < m_{\text{ES}} < 5.3$ GeV/c^2 with a B^+ signal Gaussian function and an ARGUS background function [28]. The Gaussian mean value (μ), width (σ), and the ARGUS parameter (C_{ARG}), are fixed to the values obtained when fitting m_{ES} for the entire $J/\psi\pi^+\pi^-\pi^0$ mass region separately for the B^+ and B^0 samples (for the B^+ sample $\mu = 5278.95 \pm 0.13$ MeV/c^2, $\sigma = 2.83 \pm 0.14$ MeV/c^2, and $C_{\text{ARG}} = -37.9 \pm 1.8$). A binned Poisson likelihood fit is performed to the m_{ES} distribution

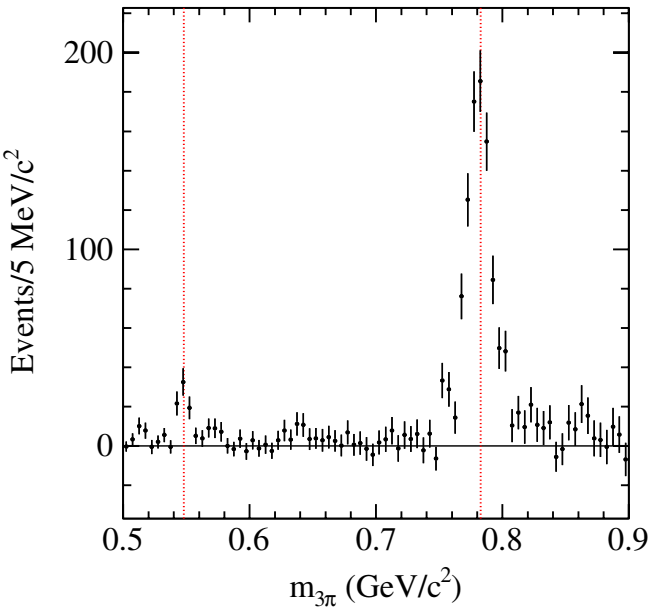

FIG. 1 (color online). The $m_{3\pi}$ distribution for $B^+ \to J/\psi\pi^+\pi^-\pi^0K^+$ candidates obtained as described in the text; the dashed vertical lines denote the central mass values of the η and ω meson [27].

in each $m_{3\pi}$ interval to obtain the Gaussian and ARGUS normalization parameter values, and hence to extract the B-meson signal.

In Fig. 1 there is a small, but clear, η-meson signal, a large ω-meson signal, and nothing of significance in between. The $J/\psi\eta$ mass distribution shows no significant structure, and will not be discussed any further.

In the ω-meson region, the signal extends down to $\sim$0.74 GeV/c^2; there is also a high-mass tail above $\sim$0.8 GeV/c^2, and possibly some small nonresonant contribution in this region. When we assign ω-Dalitz-plot weights [29] to the events in the region 0.74–0.80 GeV/c^2, the sum of weights (1030 $\pm$ 90) is consistent with the signal size (1160 $\pm$ 60), indicating that any non-ω background is small, and so we ignore such contributions. Similar behavior is observed for B^0 decay, but with a selected-event sample which is about 6 times smaller. In the following, we define the lower limit of the ω-meson mass region as 0.74 GeV/c^2, but leave the upper limit at 0.7965 and 0.8055 GeV/c^2 for the B^+ and B^0 samples [23], respectively, in order to focus on the impact of this one change on the observed $J/\psi\omega$ mass distribution. The extension of the $m_{3\pi}$ region toward lower values increases the efficiency slightly.

The $J/\psi\omega$ mass distributions for $B^{0,+} \to J/\psi\omega K^{0,+}$ candidates are obtained by using the same fit procedure used to obtain the $m_{3\pi}$ distribution. We then correct the observed signal yields for selection efficiency. Events corresponding to $B^{0,+} \to J/\psi\omega K^{0,+}$ decay are created by MC simulation, based on GEANT4 [30], in order to provide uniform coverage of the entire $m_{J/\psi\omega}$ range. The generated events are subjected to the reconstruction and selection procedures applied to the data. For B^+ (B^0) decay it is found that the efficiency increases (decreases) gradually from $\sim$6% ($\sim$5%) close to $m_{J/\psi\omega}$ threshold to $\sim$7% ($\sim$4%) for $m_{J/\psi\omega} \sim 4.8$ GeV/c^2. Comparison of generated and reconstructed $m_{J/\psi\omega}$ values within each reconstructed $m_{J/\psi\omega}$ mass interval enables the measurement of the $m_{J/\psi\omega}$ dependence of the mass resolution. From a single-Gaussian fit to each distribution, the rms deviation is found to degrade gradually from 6.5 MeV/c^2 at $m_{J/\psi\omega} \sim 3.84$ GeV/c^2, to 9 MeV/c^2 at $m_{J/\psi\omega} \sim 4.8$ GeV/c^2.

The $m_{J/\psi\omega}$ distributions for $B^+ \to J/\psi\omega K^+$ and $B^0 \to J/\psi\omega K^0$ decay, after efficiency correction in each mass interval, are shown in Figs. 2(a) and 2(b) respectively. For the latter, corrections for K^0_L production and $K^0_S \to \pi^0\pi^0$ decay have been incorporated. The $m_{J/\psi\omega}$ range from 3.8425 to 3.9925 GeV/c^2 is divided into 10 MeV/c^2 intervals, while beyond this 50 MeV/c^2 intervals are used. The same choice of intervals was used in Ref. [23], where the first two were inaccessible, and the third was only partly accessible, because of the value of the lower limit on $m_{3\pi}$. Clear enhancements are observed in the vicinity of the X and Y mesons in the B^+ distribution, and similar

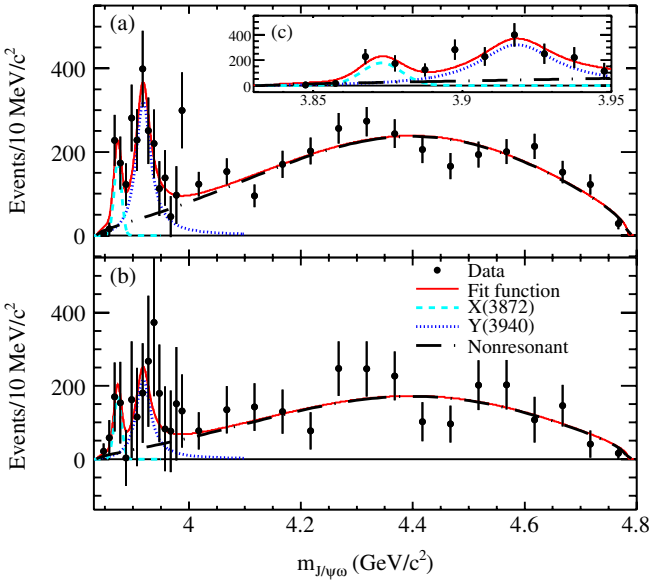

FIG. 2 (color online). The corrected $m_{J/\psi\omega}$ distribution for (a) B^+, (b) B^0 decays; (c) (inset) shows the low-mass region of (a) in detail. The curves indicate the results of the fit.

effects are present in the B^0 distribution, with lower statistical significance.

The function used to fit the distributions of Fig. 2 is a sum of three components. The X meson component is a Gaussian resolution function with fixed rms deviation $\sigma =$ 6.7 MeV/c^2 obtained from MC simulation; the intrinsic width of the X meson (estimated to be $\lesssim$ 3 MeV [27]) is ignored. The Y-meson intensity contribution is represented by a relativistic S-wave Breit-Wigner (BW) function [23]. The nonresonant contribution is described empirically by a Gaussian function multiplied by $m_{J/\psi\omega}$. The Y-meson and nonresonant intensity contributions are multiplied by the phase space factor $p \times q$, where p is the K momentum in the B rest frame, and q is the J/ψ momentum in the rest frame of the $J/\psi 3\pi$ system. A simultaneous χ^2 fit to the distributions of Figs. 2(a) and 2(b) is carried out, in which only the normalization parameters of the three contributions are allowed to differ between Figs. 2(a) and 2(b). The fit describes the data well (χ^2/NDF = 54.7/51, NDF = number of degrees of freedom), as shown by the solid curves in Fig. 2. The dashed and dotted curves show the X- and Y-meson contributions, respectively, while the dot-dashed curves represent the nonresonant distribution.

For the X meson, the fitted mass is $3873.0^{+1.8}_{-1.6}$(stat) $\pm$ 1.3(syst) MeV/c^2, while the mass and width values for the Y meson are $3919.1^{+3.8}_{-3.4}$(stat) $\pm$ 2.0(syst) MeV/c^2 and 31^{+10}_{-8}(stat) $\pm$ 5(syst) MeV, respectively. These results are consistent with earlier *BABAR* measurements [6,23].

From the fits of Fig. 2, we obtain product branching fraction measurements for $B^{0,+} \to XK^{0,+}$, $X \to J/\psi\omega$. The resulting B^+ and B^0 product branching fraction values are $[0.6 \pm 0.2(\text{stat}) \pm 0.1(\text{syst})] \times 10^{-5}$, and $[0.6 \pm 0.3(\text{stat}) \pm 0.1(\text{syst})] \times 10^{-5}$, respectively.

Similarly, we obtain updated values for $\mathcal{B}(B^+ \to YK^+) \times \mathcal{B}(Y \to J/\psi\omega) = [3.0^{+0.7}_{-0.6}(\text{stat})^{+0.5}_{-0.3}(\text{syst})] \times 10^{-5}$, $\mathcal{B}(B^0 \to YK^0) \times \mathcal{B}(Y \to J/\psi\omega) = [2.1 \pm 0.9(\text{stat}) \pm 0.3(\text{syst})] \times 10^{-5}$, and for the total (i.e. the sum of the X- meson, Y-meson, and nonresonant, contributions) $\mathcal{B}(B^+ \to J/\psi\omega K^+) = [3.2 \pm 0.1(\text{stat})^{+0.6}_{-0.3}(\text{syst})] \times 10^{-4}$ and $\mathcal{B}(B^0 \to J/\psi\omega K^0) = [2.3 \pm 0.3(\text{stat}) \pm 0.3(\text{syst})] \times 10^{-4}$. These values are consistent with those of Ref. [23], and supersede them.

We define R_X, R_Y, and R_{NR} as the ratios of the B^0 to B^+ branching fractions to the final states XK, YK, and nonresonant $J/\psi\omega K$, and extract these ratios from a simultaneous fit to the data, with the fit function adjusted to explicitly contain these parameters. This yields $R_X = 1.0^{+0.8}_{-0.6}(\text{stat})^{+0.1}_{-0.2}(\text{syst})$, $R_Y = 0.7^{+0.4}_{-0.3}(\text{stat}) \pm 0.1(\text{syst})$, and $R_{\text{NR}} = 0.7 \pm 0.1(\text{stat}) \pm 0.1(\text{syst})$. The values of R_Y and R_{NR} are consistent with those in Ref. [23]. The statistical uncertainty on R_{NR} has been reduced significantly with respect to Ref. [23] as a result of the increased luminosity, improvements in event reconstruction efficiency, but primarily through the use of much larger MC samples in the measurement of the selection efficiency as a function of $m_{J/\psi\omega}$, especially for $m_{J/\psi\omega} > 4$ GeV/c^2.

In Ref. [6], it was found that $\mathcal{B}(B^+ \to XK^+) \times \mathcal{B}(X \to J/\psi\pi^+\pi^-) = [8.5 \pm 1.5(\text{stat}) \pm 0.7(\text{syst})] \times 10^{-6}$ and $\mathcal{B}(B^0 \to XK^0) \times \mathcal{B}(X \to J/\psi\pi^+\pi^-) = [3.5 \pm 1.9(\text{stat}) \pm 0.4(\text{syst})] \times 10^{-6}$. We combine these results with those from the present analysis to obtain the ratio of the branching fractions $\mathcal{B}(X \to J/\psi\omega)/\mathcal{B}(X \to J/\psi\pi^+\pi^-)$. For B^+ (B^0) events, this ratio is 0.7 ± 0.3 (1.7 ± 1.3), where the statistical uncertainties, and those systematic uncertainties which do not cancel in the ratio, have been added in quadrature; the weighted average is 0.8 ± 0.3. This is consistent with that reported in Ref. [7] ($1.0 \pm 0.4(\text{stat}) \pm 0.3(\text{syst})$).

In obtaining the quoted systematic errors, systematic uncertainties due to tracking (2%), particle identification (4.4% and 5.2% for B^0 and B^+ events), π^0 reconstruction efficiency (3.6%), K^0_S reconstruction efficiency (2%) for the B^0 events, and $B\bar{B}$ event counting (1.1%), have been taken into account. The uncertainties on the branching fraction values for $J/\psi \to \ell^+\ell^-$ and $\omega \to 3\pi$ [27] have been treated as sources of systematic uncertainty. When fitting the m_{ES} distributions in each $m_{J/\psi\omega}$ or $m_{3\pi}$ mass interval, the parameters μ, σ, and C_{ARG} were fixed to the values obtained from the fit to the corresponding total m_{ES} distribution. Associated systematic uncertainties were estimated by increasing and decreasing the central value of each parameter by 1 standard deviation, repeating the analysis, and taking the change in each fitted quantity as an estimate of systematic uncertainty. Similarly, the systematic uncertainty associated with the efficiency-correction procedure was estimated by varying its $m_{J/\psi\omega}$ dependence within a $\pm 1\sigma$ envelope, repeating the fits to the data of Fig. 2, and taking the corresponding changes in fit parameter values as estimates of systematic uncertainty. Additional systematic uncertainties on the mass and width of the Y meson were estimated as described in Ref. [23]. The main contributions described there result from a comparison of the MC input values to those obtained after event reconstruction, and from the difference in fitted values when a P-wave BW was used instead of an S-wave BW to describe the Y-meson line shape.

Since the X-meson signal occurs at a low statistical level and at very low values of $m_{J/\psi\omega}$, there is concern that the measured signal-event yield might be biased because of the low-mass tails of the Y-meson and nonresonant contributions. A detailed MC study using samples of X-meson events ranging in size from 10–500 events showed no evidence of bias, and the spread in extracted signal yield was consistent with the corresponding statistical uncertainty obtained from the fit to the data.

We now consider the relationship between the X-meson signal and the choice of lower mass limit for the ω-meson region. In Fig. 3 we show the data corresponding to the first five mass intervals of Fig. 2 ($3.8425 < m_{J/\psi\omega} < 3.8925$ GeV/c^2) before applying the efficiency and K^0 branching fraction corrections. The points shown by open squares indicate the effect of choosing the $m_{3\pi}$ lower limit to be 0.7695 GeV/c^2 rather than 0.740 GeV/c^2. The three lowest intervals then yield no signal, and the other two contain only 11 (0.5) events in Fig. 3(a) (3(b)). This is to be compared with $42.4^{+7.8}_{-7.2}$ ($8.5^{+3.7}_{-3.0}$) events obtained when the $m_{3\pi}$ lower limit is 0.74 GeV/c^2. Since the number of events in Fig. 3 is much smaller than the total number of ω-meson events (1160 ± 60 for B^+ and 206 ± 26 for B^0 decay), and since the $m_{3\pi}$ distribution [Fig. 4(c)] differs

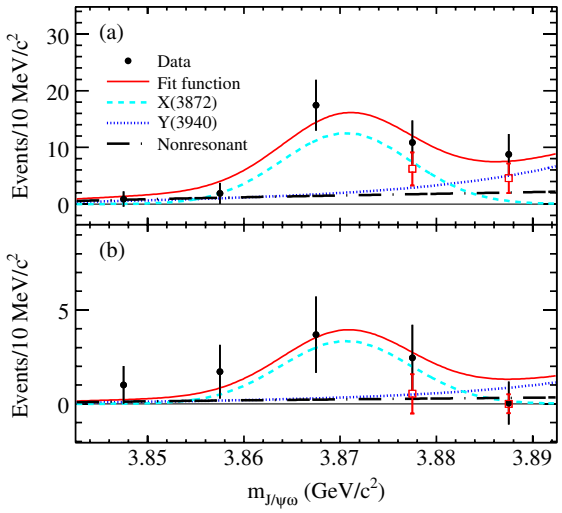

FIG. 3 (color online). The uncorrected $m_{J/\psi\omega}$ distributions for events with $3.8425 < m_{J/\psi\omega} < 3.8925$ GeV/c^2 for (a) B^+ and (b) B^0 decays; the open squares correspond to (a) $m_{3\pi} > 0.7695$ and (b) $m_{3\pi} > 0.7605$ GeV/c^2 [23]. The curves indicate the results of the fit.

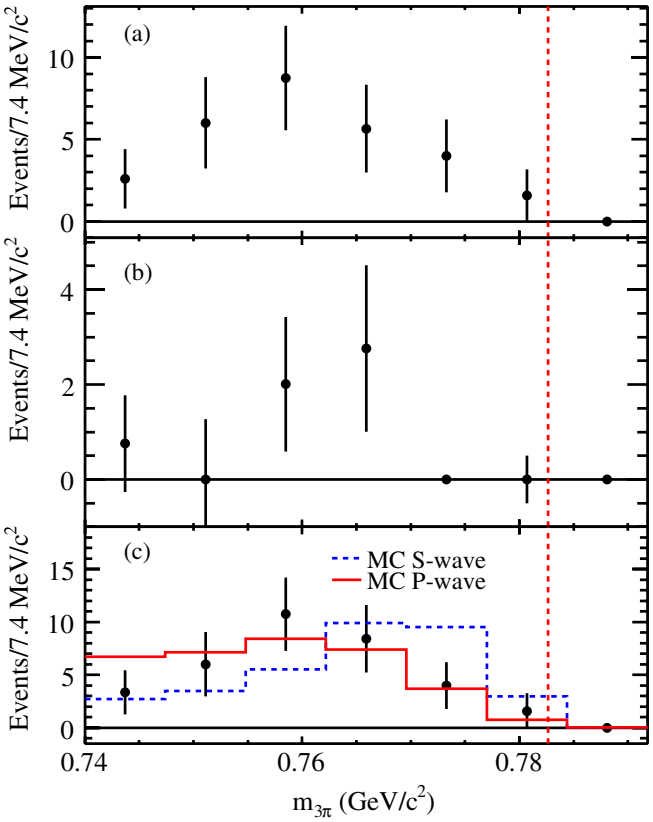

FIG. 4 (color online). The $m_{3\pi}$ distribution for events with $3.8625 < m_{J/\psi\omega} < 3.8825$ GeV/c^2 for (a) B^+, (b) B^0, and (c) the combined distribution. The vertical dashed line indicates the nominal ω-meson mass [27]. In (c), the solid (dashed) histogram represents reconstructed MC P-wave (S-wave) events normalized to the number of data events.

greatly from the ω-meson line shape, these might be nonresonant 3π events. To check the ω-meson interpretation, we sum the ω-Dalitz-plot weights [29] for the events contributing to Fig. 3(a) (solid points) in the $m_{\rm ES}$ signal region and obtain 41 ± 13, in good agreement with the number from the $m_{\rm ES}$ fits. This justifies the ω-meson interpretation. In contrast, we note that for the 152 ± 20 η-meson events in Fig. 1 the sum of the weights [29] is -1 ± 42, as expected for a uniform Dalitz-plot distribution.

To determine the significance of the $X \to J/\psi\omega$ signal, we extract the signal yields from a fit to the data, prior to the corrections for efficiency and K^0 branching fractions, as shown in Fig. 3. The fitted values of the masses and widths are in agreement with those obtained from the fit to the corrected data. An X-meson signal of 21.1 ± 7.0 events is obtained for B^+ decay, and 5.6 ± 3.0 events for B^0 decay, so that the combined signal is 26.7 ± 7.6 events. For the combined distribution, the mass region 3.8625–3.8825 GeV/c^2 contains 34.0 ± 6.6 events, and the fitted curves indicate that only 8.9 ± 1.0 events are due to the tails of the Y-meson and nonresonant distributions. We convolve a Gaussian ensemble of background Poisson distributions with a Gaussian distribution of observed events, and obtain probability 3.6×10^{-5} that the 34.0 ± 6.6 events can result from upward background fluctuation. This corresponds to a significance of 4.0σ for a normal distribution. On this basis we report evidence for the decay mode $X \to J/\psi\omega$.

For the 3.8625–3.8825 GeV/c^2 region of Fig. 3, we plot the $m_{3\pi}$ distributions in Fig. 4. Each data point results from a fit to the corresponding $m_{\rm ES}$ distribution; for the points with no error bars, the $m_{\rm ES}$ distribution is empty. For the combined distribution, Fig. 4(c), ~84% of the events have $m_{3\pi} < 0.7695$ GeV/c^2, the mass limit used in Ref. [23]. The dashed histogram in Fig. 4(c) results from normalizing the reconstructed X-meson MC events to the observed 34 events. Since the $J/\psi\omega$ system was generated with zero orbital angular momentum, this corresponds to positive X-meson parity. One unit of orbital angular momentum creates a centrifugal barrier factor $q^2/(1 + R^2q^2)$ in the description of the $J/\psi\omega$ final state, where $R = 3$ GeV^{-1} is the P-wave Blatt-Weisskopf barrier factor radius [31] (values in the range $0 < R < 5$ GeV^{-1} yield no significant difference). This factor suppresses the $\pi^+\pi^-\pi^0$ mass spectrum near the upper kinematic limit, as shown by the solid histogram of Fig. 4(c) (also normalized to 34 events). For the dashed histogram $\chi^2/\mathrm{NDF} = 10.17/5$ and the χ^2-distribution probability is $P(\chi^2, \mathrm{NDF}) = 7.1\%$, while for the solid histogram $\chi^2/\mathrm{NDF} = 3.53/5$ and $P(\chi^2, \mathrm{NDF}) = 61.9\%$. It follows that the observed distribution favors the P-wave description both quantitatively and qualitatively. If both histograms are normalized to the region $m_{3\pi} < 0.7695$ GeV/c^2 (which was excluded in Ref. [23]), we expect for $m_{3\pi} > 0.7695$ GeV/c^2, and hence for the $m_{J/\psi\omega}$ interval 3.8725–3.8825 GeV/c^2, ~4.3 events for the P-wave description, and ~16.6 events for the S-wave description. However, in Fig. 3 we observe ~6 events. In Ref. [32], it was pointed out that for $X(3872) \to D^{*0}\bar{D}^0$, the introduction of one unit of orbital angular momentum in the final state could explain the shift in measured X-meson mass [12,13]. This observation and the present analysis, together with the spin-parity (J^P) analysis of Ref. [11], favor $J^P = 2^-$ for the $X(3872)$ meson. For $I = 0$ and $J^{PC} = 2^{-+}$, the X-meson mass falls within the broad range of estimates for the $\eta_{c2}(1D)$ charmonium state [33,34]. We conclude that this interpretation is favored by the data.

In summary, we have used the entire *BABAR* data sample collected at the $\Upsilon(4S)$ resonance to obtain evidence for $X \to J/\psi\omega$ in $B^{0,+} \to J/\psi\omega K^{0,+}$ with product branching fraction values $[0.6 \pm 0.2(\mathrm{stat}) \pm 0.1(\mathrm{syst})] \times 10^{-5}$ and $[0.6 \pm 0.3(\mathrm{stat}) \pm 0.1(\mathrm{syst})] \times 10^{-5}$ for B^+ and B^0, respectively. A comparison of the observed $m_{3\pi}$ mass distribution from $X \to J/\psi\omega$ decay to those from MC simulations leads us to conclude that the inclusion of one unit of orbital angular momentum in the $J/\psi\omega$ system

significantly improves the description of the data. This in turn implies negative parity for the X meson, and hence $J^P = 2^-$ is preferred [11]. In addition, we have updated the mass and width of the Y meson $(3919.1^{+3.8}_{-3.5}(\text{stat}) \pm 2.0(\text{syst})\ \text{MeV}/c^2$ and $31^{+10}_{-8}(\text{stat}) \pm 5(\text{syst})\ \text{MeV})$, the product branching fraction values for $B^{0,+} \to YK^{0,+}$, $Y \to J/\psi\omega$, and our measurements of the total branching fractions for $B^{0,+} \to J/\psi\omega K^{0,+}$.

We are grateful for the excellent luminosity and machine conditions provided by our PEP-II colleagues, and for the substantial dedicated effort from the computing organizations that support *BABAR*. The collaborating institutions wish to thank SLAC for its support and kind hospitality. This work is supported by DOE and NSF (USA), NSERC (Canada), CEA and CNRS/IN2P3 (France), BMBF and DFG (Germany), INFN (Italy), FOM (The Netherlands), NFR (Norway), MES (Russia), MICIIN (Spain), STFC (United Kingdom). Individuals have received support from the Marie Curie EIF (European Union), the A. P. Sloan Foundation (USA), and the Binational Science Foundation (USA-Israel).

[1] S.-K. Choi *et al.*, Phys. Rev. Lett. **91**, 262001 (2003).
[2] D. E. Acosta *et al.*, Phys. Rev. Lett. **93**, 072001 (2004).
[3] V. M. Abazov *et al.*, Phys. Rev. Lett. **93**, 162002 (2004).
[4] B. Aubert *et al.*, Phys. Rev. D **71**, 071103 (2005).
[5] B. Aubert *et al.*, Phys. Rev. D **73**, 011101(R) (2006).
[6] B. Aubert *et al.*, Phys. Rev. D **77**, 111101(R) (2008).
[7] K. Abe *et al.*, arXiv:hep-ex/0505037.
[8] B. Aubert *et al.*, Phys. Rev. D **74**, 071101(R) (2006).
[9] B. Aubert *et al.*, Phys. Rev. Lett. **102**, 132001 (2009).
[10] A. Abulencia *et al.*, Phys. Rev. Lett. **96**, 102002 (2006).
[11] A. Abulencia *et al.*, Phys. Rev. Lett. **98**, 132002 (2007).
[12] G. Gokhroo *et al.*, Phys. Rev. Lett. **97**, 162002 (2006).
[13] B. Aubert *et al.*, Phys. Rev. D **77**, 011102(R) (2008).
[14] I. Adachi *et al.*, Phys. Rev. D **81**, 031103(R) (2010).
[15] F. E. Close and P. R. Page, Phys. Lett. B **628**, 215 (2005).
[16] F. E. Close, Contemp. Phys. **49**, 343 (2008).
[17] N. A. Tornqvist, Phys. Lett. B **590**, 209 (2004).
[18] E. Braaten and M. Kusunoki, Phys. Rev. D **69**, 074005 (2004).
[19] E. S. Swanson, Phys. Lett. B **588**, 189 (2004).
[20] M. B. Voloshin, Phys. Lett. B **604**, 69 (2004).
[21] M. B. Voloshin, Phys. Rev. D **76**, 014007 (2007).
[22] L. Maiani *et al.*, Phys. Rev. D **71**, 014028 (2005).
[23] B. Aubert *et al.*, Phys. Rev. Lett. **101**, 082001 (2008).
[24] S.-K. Choi *et al.*, Phys. Rev. Lett. **94**, 182002 (2005).
[25] The use of charge conjugate reactions is implied throughout this paper.
[26] B. Aubert *et al.*, Nucl. Instrum. Methods Phys. Res., Sect. A **479**, 1 (2002); W. Menges, in *Nuclear Science Symposium Conference Record* (IEEE, Piscataway, NJ, 2006), p. 1470.
[27] C. Amsler *et al.*, Phys. Lett. B **667**, 1 (2008).
[28] H. Albrecht *et al.*, Z. Phys. C **48**, 543 (1990).
[29] Each event is given weight $\frac{5}{2}(1 - 3\cos^2\theta_h)$, where θ_h is the angle between the π^+ and π^0 directions in the $\pi^+\pi^-$ rest frame.
[30] S. Agostinelli *et al.* (GEANT4 Collaboration), Nucl. Instrum. Methods Phys. Res., Sect. A **506**, 250 (2003).
[31] J. M. Blatt and V. F. Weisskopf, *Theoretical Nuclear Physics* (John Wiley & Sons, New York, 1952).
[32] W. Dunwoodie and V. Ziegler, Phys. Rev. Lett. **100**, 062006 (2008).
[33] S. Godfrey and N. Isgur, Phys. Rev. D **32**, 189 (1985).
[34] E. Eichten *et al.*, Rev. Mod. Phys. **80**, 1161 (2008).